

Feast Your Eyes: Mixture-of-Resolution Adaptation for Multimodal Large Language Models

Gen Luo^{1,2} Yiyi Zhou^{1,3} Yuxin Zhang^{1,3} Xiawu Zheng^{1,3} Xiaoshuai Sun^{1,3} Rongrong Ji^{1,3}

Abstract

Despite remarkable progress, existing multimodal large language models (MLLMs) are still inferior in granular visual recognition. Contrary to previous works, we study this problem from the perspective of image resolution, and reveal that a combination of low- and high-resolution visual features can effectively mitigate this shortcoming. Based on this observation, we propose a novel and efficient method for MLLMs, termed *Mixture-of-Resolution Adaptation* (MRA). In particular, MRA adopts two visual pathways for images with different resolutions, where high-resolution visual information is embedded into the low-resolution pathway via the novel *mixture-of-resolution adapters* (MR-Adapters). This design also greatly reduces the input sequence length of MLLMs. To validate MRA, we apply it to a recent MLLM called LLaVA, and term the new model *LLaVA-HR*. We conduct extensive experiments on 11 vision-language (VL) tasks, which show that LLaVA-HR outperforms existing MLLMs on 8 VL tasks, *e.g.*, +9.4% on TextVQA. More importantly, both training and inference of LLaVA-HR remain efficient with MRA, *e.g.*, **20 training hours** and **3× inference speed** than LLaVA-1.5. Source codes are released at: <https://github.com/luogen1996/LLaVA-HR>.

1. Introduction

Driven by the remarkable success of large language models (LLMs) (Touvron et al., 2023; Chen et al., 2020), research on multi-modal large language models (MLLMs) also receives an influx of interest in the machine learning community (Liu et al., 2023b; Luo et al., 2023a; Alayrac et al.,

¹Key Laboratory of Multimedia Trusted Perception and Efficient Computing, Ministry of Education of China, School of Informatics, Xiamen University, 361005, P.R. China ²Peng Cheng Laboratory, Shenzhen, 518000, China ³Institute of Artificial Intelligence, Xiamen University, 361005, P.R. China. Correspondence to: Rongrong Ji <rrji@xmu.edu.cn>.

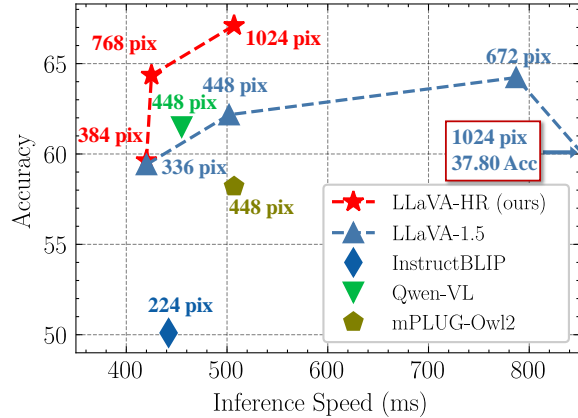


Figure 1. Zero-shot performance and inference speed of LLaVA-HR and existing MLLMs on TextVQA. Existing MLLMs often fall short of fine-grained VL tasks like TextVQA. Increasing image resolution is an effective yet expensive solution. With the proposed MRA, our LLaVA-HR can efficiently adopt high-resolution images to boost performance.

2022; Chen et al., 2022; 2023b). Numerous efforts have been recently devoted to extending LLMs to more modalities, achieving breakthroughs on various vision-language tasks (Goyal et al., 2017; Singh et al., 2019; Hudson & Manning, 2019). Despite advances, existing MLLMs still fall short of granular visual recognition. For instance, the powerful GPT4-V also suffers from hallucinations when identifying small and occluded objects (Tong et al., 2024). This shortcoming inevitably limits the practical use of MLLMs.

To compensate for this shortcoming, practitioners often resort to scaling up model size and increasing per-training data size (Alayrac et al., 2022; Li et al., 2023b; Bai et al., 2023). For instance, InstructBLIP (Dai et al., 2023) adopts over 129M image-text pairs for vision-language (VL) alignments, and shows that a larger visual encoder is beneficial for MLLMs. Motivated by this, Qwen-VL (Bai et al., 2023) further increases the parameters of visual encoder to 1.9 billion and uses 1.5 billion pre-training data. Despite progress, this paradigm is prohibitively expensive, which often consumes about thousands of GPU hours.

Orthogonal to these works, we study the visual shortcoming of MLLMs from the perspective of input image resolutions. As revealed in previous VL research (Jiang et al., 2020; Tong

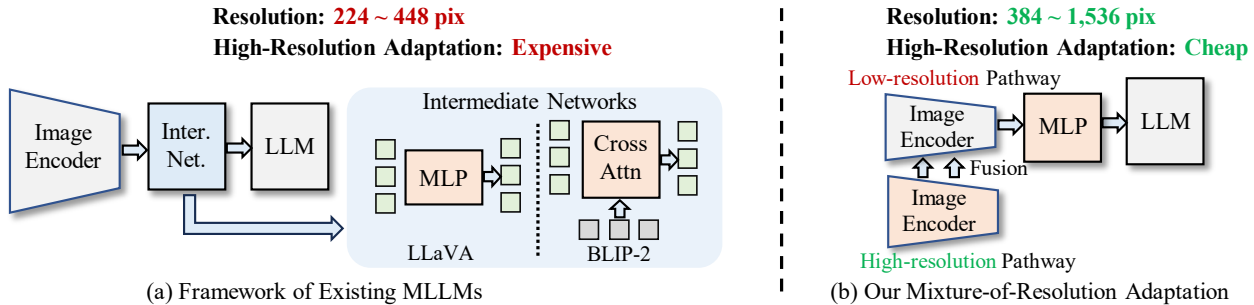


Figure 2. Comparison between existing MLLMs and LLaVA-HR. Due to high computation complexity, existing MLLMs (Liu et al., 2023a; Li et al., 2023b) often use input images of low-resolution, which are insufficient for granular visual reasoning. With our mixture-of-resolution adaptation, the proposed LLaVA-HR can increase the image resolution up to $1,536 \times 1,536$ with limited additional costs.

et al., 2024; Luo et al., 2023b), increasing the resolution of input images is a straightforward solution to improve visual recognition, which becomes more important for MLLMs that involve *visual chain-of-thought* (Rose et al., 2023). As shown in Fig. 1, increasing the resolution of LLaVA-1.5 (Liu et al., 2023a) from 384×384 to 672×672 can bring obvious performance gains (+4.6%) on TextVQA (Singh et al., 2019). However, the use of high-resolution images will greatly exacerbate the already high computational cost of MLLMs. For instance, 448×448 resolution will increase the computation complexity of LLaVA by about 1.4 times compared with the default 336×336 . In addition, due to the complex structure of MLLMs, the training will become unstable as the resolution is greatly increased, e.g., a sharp drop at $1,022 \times 1,022$ resolution, as shown in Fig. 1. We assume that the length of visual sequences greatly exceeds the pre-trained context length, leading to training instability.

In this paper, we propose a novel and efficient method for the high-resolution image adaptation of MLLMs, namely *mixture-of-resolution adaptation* (MRA). As shown in Fig. 1, MRA adopts an innovative dual visual pathway design to process the input images of high- and low-resolutions simultaneously. Specifically, one pathway aims to encode global information of low-resolution images, while the other one serves to capture fine-grained semantics from high-resolution images. Meanwhile, these two pathways are closely interacted via the novel *mixture-of-resolution adapters* (MR-Adapters), which embeds the high-resolution visual information into the low-resolution modeling. In this way, we can use a much fewer number of visual tokens to represent the input images from macro- to micro-views. With the careful design of dual-pathway structure, MRA can easily increase the image resolution up to $1,536 \times 1,536$ pixels while maintaining high efficiency.

To validate MRA, we apply it to a recent MLLM called LLaVA (Liu et al., 2023b;a), and term the new model as LLaVA-HR. We conduct extensive experiments on 11 vision-language (VL) tasks, including common VL tasks like VQA2.0 (Goyal et al., 2017) and emerging benchmarks

such as POPE (Li et al., 2023c). Experimental results show that LLaVA-HR outperforms existing MLLMs on 8 of 11 VL tasks, e.g., +9.6% over LLaVA-1.5 on TextVQA. More importantly, the training and inference of LLaVA-HR are cost-effective. The pre-training and instruction tuning of LLaVA-HR (7B, $1,024 \times 1,024$) only take a total of 20.7 hours on 8 A800 GPUs, which is *hundreds of times cheaper* than InstructBLIP (Dai et al., 2023) and Qwen-VL (Bai et al., 2023). With the same resolution, its inference speed is *3 times faster* than LLaVA-1.5 (Liu et al., 2023a).

In summary, our contributions are three folds:

- We reveal the significance of image resolution for MLLMs and propose a novel and efficient adaptation scheme, termed *mixture-of-resolution adaptation* (MRA), which adopts a novel dual visual pathway design to obtain the benefits of high-resolution visual information while keeping training and inference efficient.
- We propose a novel *mixture-of-resolution adapter* (MR-Adapter) for MRA, which can embed the high-resolution information into the low-resolution visual pathway to improve visual descriptive power.
- Based on MRA, we propose a powerful MLLM, coined LLaVA-HR, which outperforms existing MLLMs on 8 of 11 VL tasks and spends much cheaper training expenditure than most MLLMs.

2. Related Work

2.1. Multimodal Large Language Models

Driven by the great successes of large language models (LLMs) (Gilardi et al., 2023; Touvron et al., 2023; Chen et al., 2020), growing interest has been aroused in building end-to-end multimodal large language models (MLLMs) (Liu et al., 2023b; Zhu et al., 2023; Luo et al., 2023a; Fuyu-8B, 2023; Peng et al., 2023; Liu et al., 2023c). In particular, most existing MLLMs adopt a modular structure (Luo et al., 2023a; Liu et al., 2023b), which utilizes

an intermediate network to project the visual features into the word embedding space of the LLM. Then, the LLM is used to accomplish various VL tasks in an autoregressive manner. Based on the modular structure, existing MLLMs can be distinguished by the designs of the intermediate network. Popular MLLMs represented by LLaVA (Liu et al., 2023b) often adopt a linear projection layer or an MLP layer to connect the visual encoder and the LLM (Liu et al., 2023b;a; Chen et al., 2023a;b; Peng et al., 2023). The other works employ sampler-based modules to bridge the gap between the visual encoder and the LLM (Bai et al., 2023; Alayrac et al., 2022; Li et al., 2023b; Dai et al., 2023). These sampler-based modules can effectively reduce the number of visual tokens, but often requires a large-scale pre-training to achieve a promising performance (Bai et al., 2023; Li et al., 2023b). Despite the effectiveness, most existing MLLMs still adopt a low visual resolution, e.g., 336×336 , which greatly limits their performance in fine-grained tasks.

2.2. Visual Representations for MLLMs

The pursuit of better visual representations has been a popular research trend in the VL community (Lu et al., 2019; Jiang et al., 2020; Radford et al., 2021; Ren et al., 2024). Early endeavors mainly explore the object-level features for VL models (Lu et al., 2019; Zhang et al., 2021). Driven by the large-scale image-text pre-training, grid features from CLIP (Radford et al., 2021) have demonstrated the great efficiency and generalization in MLLMs (Liu et al., 2023b; Chen et al., 2022; Alayrac et al., 2022). Based on grid features, existing researchers mainly improve visual representations by scaling up the visual encoder. For example, PaLI (Chen et al., 2022) increases the parameters of visual encoder to 3 billions and shows the significant performance boost of MLLMs. In contrast to these works, we improve the visual representations for MLLMs from the perspective of image resolution, and propose a novel and efficient solution, namely mixture-of-resolution adaptation.

3. Preliminary

We first recap the structure of multimodal large language models (MLLMs), which consists of an image encoder $\mathcal{F}_{\mathcal{I}}(\cdot)$, an intermediate network $\mathcal{F}_{\mathcal{P}}(\cdot)$ and an LLM $\mathcal{F}_{\mathcal{L}}(\cdot)$.

In particular, given an input image $I \in \mathbb{R}^{H \times W \times 3}$ and a textual instruction $T \in \mathbb{R}^L$, the visual tokens $\mathbf{F}_v \in \mathbb{R}^{(h \times w) \times d}$ are obtained via the image encoder, and the text tokens $f_t \in \mathbb{R}^{l \times d}$ are represented by the corresponding word embeddings. Based on the visual and textual tokens, the LLM will decode the target word step by step, formulated as

$$p_t = \prod_{s=1}^{S+1} \mathcal{F}_{\mathcal{L}}(R_s | \mathcal{F}_{\mathcal{P}}(\mathbf{F}_v), f_t, R_{0:s-1}). \quad (1)$$

Here, $p_t \in \mathbb{R}^m$ denotes the probabilities of the predicted word and m is the size of word vocabulary.

In some MLLMs (Liu et al., 2023b;a), $\mathcal{F}_{\mathcal{P}}(\cdot)$ is often a stack of simple linear layers, which are used to directly project the visual tokens onto the semantic space of LLMs. Although simple and effective, this strategy inevitably leads to a longer visual sequence as the resolution increases, e.g., 5,329 tokens for $1,022 \times 1,022$ resolution in LLaVA-1.5. In practice, processing such a large number of tokens is computationally expensive in MLLMs. To further reduce the number of visual tokens, recent advances adopt the sampler-based module for $\mathcal{F}_{\mathcal{P}}(\cdot)$, e.g., *QFormer* (Li et al., 2023b), which aggregates visual features into several tokens that LLM can directly handle. Nevertheless, these methods often require large-scale pre-training to achieve VL alignments (Bai et al., 2023; Li et al., 2023b).

Based on the above analyses, we conclude that the main difficulty of high-resolution image adaptation lies in the rapidly growing visual sequence. This issue motivates us to further explore how to efficiently encode richer visual information with fewer visual tokens.

4. Mixture-of-Resolution Adaptation

4.1. Overview

To address the above issues, we propose a novel and efficient method for MLLMs, termed *mixture-of-resolution adaptation* (MRA), of which structure is depicted in Fig. 3. The core idea of MRA is to embed high-resolution information into the low-resolution one via a dual pathway design. In this case, MRA can keep a smaller number of visual tokens while encoding richer visual information.

Particularly, given the input images of two resolutions $I_l \in \mathbb{R}^{H_l \times W_l \times 3}$ and $I_h \in \mathbb{R}^{H_h \times W_h \times 3}$, the process of MRA can be formulated as

$$\begin{aligned} \mathbf{F}_v &= \mathcal{F}_{\mathcal{I}_l}(I_l, \mathcal{F}_{\mathcal{A}}(\mathbf{F}_{vh})) + \mathbf{F}_{vh}, \\ \mathbf{F}_{vh} &= \mathcal{F}_{\mathcal{I}_h}(I_h). \end{aligned} \quad (2)$$

Here, $\mathbf{F}_{vh} \in \mathbb{R}^{h_h \times w_h \times d_h}$ and $\mathbf{F}_v \in \mathbb{R}^{h \times w \times d}$ denote the high-resolution features and the final visual features, respectively. And $\mathcal{F}_{\mathcal{I}_l}$ and $\mathcal{F}_{\mathcal{I}_h}$ are the visual encoders for high-resolution and low-resolution images, respectively. $\mathcal{F}_{\mathcal{A}}$ denotes the *mixture-of-resolution adapter* (MR-Adapter). In Eq. 2, MRA adopts dual visual pathways to process high- and low- resolution images simultaneously. Then, a novel MR-Adapter is used to fuse the high-resolution information from the slow pathway to the fast one. Finally, the visual features of two resolutions are combined and processed by the LLM based on Eq. 1.

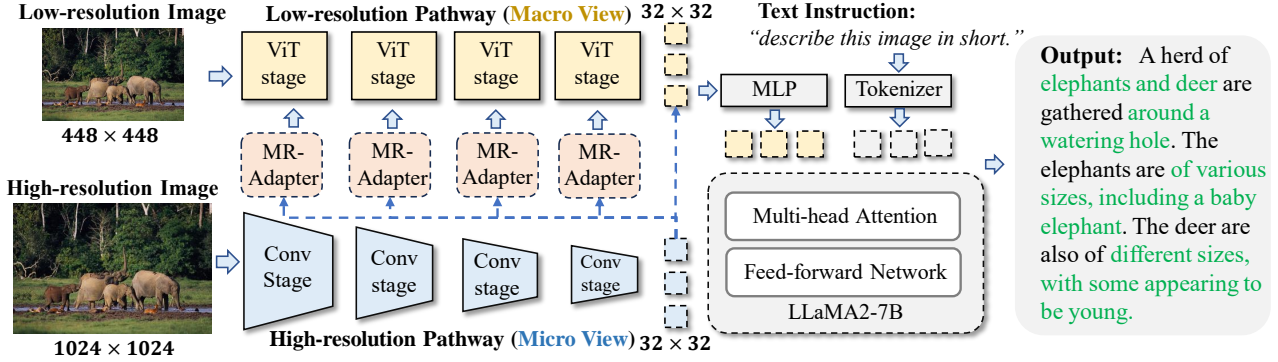


Figure 3. Illustration of Mixture-of-Resolution Adaptation (MRA) and its deployment on LLaVA-HR. MRA employs dual visual pathways to process high-resolution and low-resolution images, respectively. High-resolution information is embedded into the fast pathway via a novel mixture-of-resolution adapter (MR-Adapter).

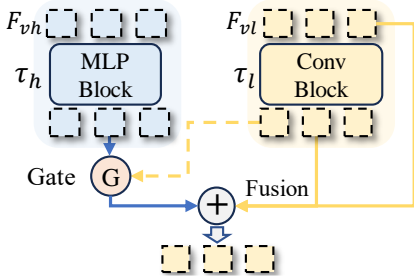


Figure 4. Illustration of the mixture-of-resolution adapter (MR-Adapter). MR-Adapter can dynamically embed the high-resolution features into the low-resolution pathway.

4.2. Dual Visual Pathways

As shown in Fig. 3, dual visual pathways are the key design of MRA, and their benefits are maximized from two aspects.

Visual functionality. Firstly, the dual visual pathways process images from macro- and micro-views, which is inspired by the visual system of human being (Merigan & Maunsell, 1993; Robertson & Lamb, 1991). Particularly, Robertson & Lamb (1991) find that the visual system processes local and global semantics via different pathways. Based on this finding, we adopt a similar mechanism to our MRA. Specifically, one visual pathway aims to capture fine-grained semantics from high-resolution images *i.e.*, processing images from local view. In contrast, the other pathway is designed to encode global information from low-resolution images, achieving a larger receptive field.

Visual alignment. Due to different resolutions, these two pathways often produce visual features of different shapes, impeding their quick alignments (Yu et al., 2019). To overcome this limitation, we adopt different downsampling rates for the low- and high-resolution pathways, respectively. Thus, their output features can keep the same spatial shape.

Based on the above observations, we design the dual visual pathways with a convolutional network (CNN) (Liu et al., 2022) and a vision transformer (ViT) (Dosovitskiy et al.,

2020). Specifically, CNN is equipped with a downsampling stride of 32 to process high-resolution images. ViT encodes low-resolution images with a downsampling stride of 14. Notably, such designs also ensure the efficiency of MLLMs, where the high-resolution images are processed by the efficient CNN, and the number of visual tokens is also kept small via the large downsampling stride.

4.3. Mixture-of-Resolution Adapter

To better collaborate the feature learning of two pathways, we propose a *mixture-of-resolution adapter* (MR-Adapter) for the fusion of visual information from different resolution images. In particular, given the visual features $\mathbf{F}_{vh} \in \mathbb{R}^{h \times w \times d_h}$ extracted from a high-resolution image, we embed them into the low-resolution visual pathway by

$$\mathbf{F}'_{vl} = \mathbf{F}_{vl} + f_l(\mathbf{F}_{vl}) + g \cdot f_h(\mathbf{F}_{vh}). \quad (3)$$

Here, $\mathbf{F}_{vl} \in \mathbb{R}^{h \times w \times d_l}$ are the features from the low-resolution pathway. $f_l(\cdot)$ and $f_h(\cdot)$ denote two mapping modules, which are designed as a convolutional block and an MLP layer, respectively. g is a dynamic score to control the weights of high-resolution information, defined by

$$g = \delta(W_2 \sigma(W_1 f_v)),$$

$$f_v = \frac{1}{h \times w} \sum_i^h \sum_j^w [f_l(\mathbf{F}_{vl})^{i,j}, f_h(\mathbf{F}_{vh})^{i,j}]. \quad (4)$$

Here, $[\cdot]$ denotes the concatenation operation, and $W_1 \in \mathbb{R}^{2d \times \frac{d}{2}}$ and $W_2 \in \mathbb{R}^{\frac{d}{2} \times d}$ are two projection matrices. $f_v \in \mathbb{R}^d$ is the pooled visual features. σ and δ denote the activation function of *GELU* and *Tanh*, respectively.

As shown in Fig. 3, high-resolution information can be fused with the features in each block of ViT. In this case, the low-resolution features of ViT also contain rich semantics, improving the visual descriptive power of MLLMs.

Table 1. Performance and efficiency comparisons of LLaVA-HR and LLaVA-1.5 (Liu et al., 2023a) at different resolutions. Except resolution, the other configurations of LLaVA-HR and LLaVA-1.5 remain the same. The training and inference costs are measured on NVIDIA A800s. “N/A” denotes that GPU memory overflows¹. “tokens/s” denotes the number of generated tokens per second.

Models	Resolution	Vision-Language Tasks				Training	GPU	Inference
		VQAv2 \uparrow	TextVQA \uparrow	MME \uparrow	POPE \uparrow	Time \downarrow	Memory \downarrow	Speed \uparrow
LLaVA-1.5	336 pix	80.44	59.41	1461.17	86.2	15.6h	28G	23.8 tokens/s
LLaVA-HR (ours)	384 pix	80.47	59.63	1522.28	86.3	17.6h	34G	23.8 tokens/s
LLaVA-1.5	448 pix	81.17	62.17	1493.12	87.2	19.4h	49G	19.9 tokens/s
LLaVA-HR (ours)	768 pix	81.80	64.36	1524.75	88.0	18.2h	38G	23.5 tokens/s
LLaVA-1.5	672 pix	81.54	64.23	1498.71	87.9	31.8h	79G	12.7 tokens/s
LLaVA-HR (ours)	1024 pix	81.90	67.11	1554.90	87.6	20.7h	40G	19.7 tokens/s
LLaVA-1.5	1022 pix	74.20	37.80	1266.90	84.4	69.4h	N/A ¹	5.6 tokens/s
LLaVA-HR (ours)	1536 pix	81.82	67.96	1480.62	87.7	29.8h	52G	12.6 tokens/s

4.4. The Deployment on MLLM

We apply MRA to a popular MLLM called LLaVA-1.5 (Liu et al., 2023a), and construct a new model, namely LLaVA-HR. Its training consists of two stages, *i.e.*, low-resolution pre-training and high-resolution instruction tuning.

Stage 1: Low-Resolution Pre-training. Similar to LLaVA (Liu et al., 2023b) and LLaVA-1.5 (Liu et al., 2023a), this stage aims to optimize the projector to align the visual features with the word embeddings of LLM. Therefore, the image encoder and the LLM are frozen during pre-training. Besides, we adopt low resolutions for two pathways. In this stage, the MR-Adapter is not inserted, and output features of dual pathways are directly combined.

Stage 2: High-Resolution Instruction Tuning. During instruction tuning, we greatly increase the resolution of the high-resolution pathway, *e.g.*, from 384×384 to $1,024 \times 1,024$. And the low-resolution one is also accordingly adjusted to ensure the visual alignment of two pathways, *e.g.*, from 336×336 to 448×448 . Meanwhile, the MR-Adapter is then applied to connect two visual pathways. Different from the first training stage, the entire MLLM will be fully optimized to better accommodate high-resolution images.

5. Experiments

5.1. Evaluations and Metrics

Multimodal benchmarks for MLLM. We evaluate LLaVA-HR on four emerging multimodal benchmarks for MLLMs, including MME (Fu et al., 2023), POPE (Li et al., 2023c), SEED (Li et al., 2023a) and MM-VET (Yu et al., 2023). In particular, MME and MM-VET evaluate the multimodal per-

¹When memory overflows, we reduce the batch size and increase the gradient accumulation steps to train LLaVA-1.5.

ception and cognition abilities of MLLMs. SEED extends the modalities of evaluation to images and videos. POPE aims to evaluate the visual hallucinations of MLLMs. The metrics used in our paper follow their default settings. For MME, we follow LLaVA-1.5 to report the perception score.

Common vision-language benchmarks. We also evaluate LLaVA-HR on seven VL datasets, including VQAv2 (Goyal et al., 2017), GQA (Hudson & Manning, 2019), OKVQA (Marino et al., 2019), OCRVQA (Mishra et al., 2019), ScienceQA (Lu et al., 2022), VizWiz (Gurari et al., 2018) and TextVQA. In particular, ScienceQA (Lu et al., 2022), VizWiz (Gurari et al., 2018) and TextVQA are three **zero-shot tasks**, and their samples are not appeared in our training data. We report the accuracy on the *test* set of OCRVQA, the *test* set of VizWiz, and the *val* set of OKVQA. We organize samples of these tasks in instruction formats of LLaVA-1.5 (Liu et al., 2023a).

5.2. Implementation Details

In LLaVA-HR, we use CLIP-ViT-L (Radford et al., 2021; Ilharco et al., 2021) and CLIP-ConvNeXt-L (Liu et al., 2022) as the dual visual paths to encode low- and high-resolution images, respectively. In LLaVA-HR-X, the CLIP-ConvNeXt-L is replaced with the stronger CLIP-ConvNeXt-XXL. The MR-Adapter is applied into the last three stages of ViT. Following LLaVA-1.5, we first pre-train LLaVA-HR on LCS-558K (Liu et al., 2023b), which contains 558k image-text pairs. During the pre-training stage, both the visual encoder and the LLM are frozen, and only the MLP projector is fine-tuned. AdamW (Kingma & Ba, 2014) is used as the optimizer, and the learning rate and batch size are set to $1e-3$ and 256, respectively. Visual resolutions are set to 336×336 and 384×384 for the ViT and the CNN, respectively. During instruction tuning, we follow LLaVA-1.5 to use 665k VL instruction data. At this stage, the entire

Table 2. Comparison of MRA and four baselines on LLaVA-HR. The visual resolution is set to about $\sim 760 \times 760$.

Settings	VQAv2	TextVQA	MME	POPE	Speed
ViT+ MLP	81.0	63.2	1436.1	87.6	10.7 t/s
Conv+MLP	80.3	64.6	1415.9	86.6	23.7 t/s
ViT+Resampler	79.8	58.9	1403.8	85.8	27.6 t/s
ViT+Pooling+MLP	80.6	59.6	1480.6	86.5	23.9 t/s
MRA (ours)	81.8	64.4	1524.8	88.0	23.5 t/s

model is updated with a learning rate of $2e-5$. Besides, we increase the resolution of ViT and CNN to 448×448 and $1,024 \times 1,024$, respectively. The training epoch is set to 1 for pre-training and instruction tuning.

5.3. Experimental Results

5.3.1. QUANTITATIVE ANALYSIS

Comparison with baselines. In Tab. 1, we compare the performance and efficiency of LLaVA-HR with LLaVA-1.5 (Liu et al., 2023a) with different image resolutions. From this table, we observe that increasing image resolution obviously improves the performance of two models on four tasks, *e.g.*, +4.8% of LLaVA-1.5 on TextVQA. However, the performance of LLaVA-1.5 drops significantly at the resolution of $1,024 \times 1,024$. To explain, the number of visual tokens greatly exceeds the pre-trained context length of the LLM, which easily causes the instability during training. In contrast, the performance of LLaVA-HR is consistently improved from 384×384 resolution to $1,024 \times 1,024$ resolution. Besides, the total gain of LLaVA-HR is more obvious than that of LLaVA-1.5 (Liu et al., 2023a), *e.g.*, +8.33% of LLaVA-HR vs. +4.82% of LLaVA-1.5, greatly confirming the effectiveness of MRA.

In Tab. 2, we further compare four common baselines with the similar resolution, *i.e.*, $\sim 760 \times 760$. “ViT+MLP” is the default setting of LLaVA-1.5 as the reference. “Conv+MLP” replaces the visual backbone with ConvNeXt (Liu et al., 2022), which uses a larger downsampling rate to reduce the number of visual tokens. “ViT+Resampler” and “ViT+Pooling+MLP” refer to the two pooling strategies for reducing the number of visual tokens. As can be seen, all compared methods are inferior to LLaVA-HR. In particular, using a convolutional network as the visual backbone greatly improves efficiency, but its performance still lags behind LLaVA-HR by a large margin, *e.g.*, -108.9 on MME (Fu et al., 2023). Similarly, “ViT+Resampler” and “ViT+Pooling+MLP” also sacrifice performance for efficiency. Overall, these comparisons further confirm the designs of MRA.

Despite effectiveness, the expenditure of LLaVA-HR is also cost-effective. In particular, increasing resolution from 384

Table 3. Ablation study of mixture-of-resolution adaptation on LLaVA-HR. The resolution is 768×768 . Our final setting is colored in gray. “L-Res Path.,” “H-Res Path.,” “Fusion Direct.,” “Struct.” and “Gate Fuct.” denote the low-resolution pathway, the high-resolution pathway, the fusion direction, the structure and the gate function, respectively.

Settings	Choices	VQAv2	TextVQA	MME	POPE
L-Res Path.	ViT-L	81.8	64.4	1524.8	88.0
	None	80.3	64.6	1415.9	86.6
	ViT-G	81.7	65.3	1469.7	87.9
H-Res Path.	ConvNeXt-L	81.8	64.4	1524.8	88.0
	None	80.4	59.4	1461.2	86.2
	ConvNeXt-XXL	82.3	66.5	1479.2	87.9
Fusion Direct.	High to Low	81.8	64.4	1524.8	88.0
	Low to High	81.0	62.8	1463.5	87.3
Fusion Type	Sum	81.8	64.4	1524.8	88.0
	Concat	81.7	64.7	1508.8	87.3
Struct.	mlp-conv	81.8	64.4	1524.8	88.0
	conv-conv	81.6	64.6	1499.0	87.7
	conv-mlp	81.5	64.2	1517.9	87.6
Gate Funct.	Tanh	81.8	64.4	1524.8	88.0
	Sigmoid	81.7	64.3	1567.9	86.9
	H-sigmoid	81.6	64.4	1525.9	87.8

$\times 384$ to $1,024 \times 1,024$ slows down the training and inference of LLaVA-1.5 by 344.8% and 325%, respectively. However, these costs are reduced to only 17.6% and 20.8% in LLaVA-HR. Despite better performance, the training and inference speeds of LLaVA-HR are three times faster than LLaVA-1.5. Besides, the costs of GPU memory also remain cheap for LLaVA-HR. For example, adapting the resolution of $1,536 \times 1,536$ for LLaVA-HR only consumes 52G GPU memory, but the same settings for LLaVA-1.5 will cause GPU memory overflow. These results greatly confirm the efficiency of our MRA and LLaVA-HR.

Ablation studies. In Tab. 3, we conduct comprehensive ablation studies for MRA on four VL benchmarks. Firstly, we validate the different designs of the dual visual pathways. From these results, we find that removing one pathway will lead to significant performance drops, *e.g.*, -1.5% on VQAv2. Besides, scaling up the high-resolution encoder brings more gains than that of the low-resolution one, *e.g.*, +2.1% vs. +0.9% on TextVQA. We assume that the stronger high-resolution image encoder can better capture the fine-grained visual information. Then, we ablate different fusion directions and strategies in MRA. Specifically, changing the fusion direction obviously degenerates the performance, *e.g.*,

Table 4. Comparison with existing methods on four MLLM benchmarks. “Param.,” “Res.,” and “Data” refer to the total parameters, the visual resolution and the number of training data, respectively. “t/s” refers to tokens per second.

Method	Settings			Multimodal Benchmarks				Inference
	Param.	Res.	Data	MME	POPE	SEED	MM-Vet	Speed
BLIP-2	14.2B	224	129M	1293.8	85.3	46.4	22.4	-
InstructBLIP	8.2B	224	130M	-	-	53.4	26.2	22.6 t/s
InstructBLIP	14.2B	224	130M	1212.8	78.9	-	25.6	-
QWen-VL-Chat	9.6B	448	1.4B	1487.5	-	58.2	-	17.0 t/s
Fuyu-8B	8B	~600	-	728.6	74.1	-	21.4	15.6 t/s
mPLUG-Owl2	8.2B	448	400M	1450.2	-	57.8	36.2	19.6 t/s
LLaVA-1.5	7.2B	336	1.2M	1510.7	85.9	58.6	30.5	23.8 t/s
LLaVA-1.5	13.2B	336	1.2M	1531.3	85.9	61.6	35.4	-
LLaVA-HR	7.4B	1024	1.2M	1554.9	87.6	64.2	31.2	19.7 t/s
LLaVA-HR	13.4B	1024	1.2M	1540.9	87.8	64.5	34.8	15.0 t/s
LLaVA-HR-X	14B	1024	1.2M	1487.3	88.0	65.3	35.5	12.9 t/s

 Table 5. Comparison with existing methods on seven vision-language tasks. SQA^I refers to the IMG subset of ScienceQA.

Method	Settings			In-domain Tasks				Zero-shot Tasks			Infer.
	Param.	Res.	Data	VQAv2	GQA	OKVQA	OCRvQA	SQA ^I	VizWiz	TextVQA	Speed
BLIP-2	14.2B	224	129M	41.0	41.0	45.9	40.6	61.0	19.6	42.5	-
InstructBLIP	8.2B	224	130M	-	49.2	-	-	60.5	34.5	50.1	22.6 t/s
InstructBLIP	14.2B	224	130M	-	49.5	-	44.8	63.1	33.4	50.7	-
Shikra	13.2B	224	6.1M	77.4	-	-	-	-	-	-	-
IDEFICS-9B	9B	224	354M	50.9	-	38.4	-	-	35.5	25.9	30.5 t/s
IDEFICS-80B	80B	224	354M	60.0	-	45.2	-	-	36.0	30.9	-
Qwen-VL-Chat	9.6B	448	1.4B	78.2	57.5	56.6	70.5	68.2	38.9	61.5	17.0 t/s
Fuyu-8B	8B	~600	-	74.2	-	60.6	-	-	-	-	15.6 t/s
mPLUG-Owl2	8.2B	448	400M	79.4	56.1	57.7	-	68.7	54.5	58.2	19.6 t/s
LLaVA-1.5	7.2B	336	1.2M	78.5	62.0	-	-	66.8	50.0	58.2	23.8 t/s
LLaVA-1.5	13.2B	336	1.2M	80.0	63.3	-	-	71.6	53.6	61.3	-
LLaVA-HR	7.4B	1024	1.2M	81.9	64.2	58.9	68.4	65.1	48.7	67.1	19.7 t/s
LLaVA-HR	13.4B	1024	1.2M	82.3	64.8	60.7	67.7	68.1	57.9	68.1	15.0 t/s
LLaVA-HR-X	14B	1024	1.2M	82.6	65.2	61.5	69.0	68.0	56.6	70.9	12.9 t/s

-61.3 on MME. Finally, we ablate the designs of the mixture-of-resolution adapter. Specifically, the best choices of mapping modules for the low- and high-resolution pathways are convolution blocks and MLP blocks, respectively. Besides, the choices of gating function also affect performance and the \tanh function perform the best. These ablations further confirm the designs of MR-Adapter.

Comparison with existing MLLMs. In Tab. 4 - 5, we compare LLaVA-HR with existing MLLMs on 11 VL tasks. On the four MLLM benchmarks, we observe comprehensive advantages of LLaVA-HR against existing MLLMs. In particular, LLaVA-HR achieves 1554.9 scores in MME benchmark, outperforming LLaVA-1.5 by +23.6. On POPE, a benchmark including video evaluations, LLaVA-HR-X still outperforms existing MLLMs by a large margin, *i.e.*, +3.7% gains. Besides, LLaVA-HR achieves the best per-

formance on the benchmark for visual hallucinations, *i.e.*, POPE, suggesting that its visual hallucinations are greatly alleviated. Notably, Fuyu-8b (Fuyu-8B, 2023) is capable of high-resolution images, but its performance is much inferior to LLaVA-HR, *e.g.*, 728.6 vs. 1554.9 on MME.

Tab. 5 gives the performance comparison on common VL tasks. On in-domain tasks, LLaVA-HR achieves the best results on three tasks, *e.g.*, 82.6 on VQAv2 and 61.5 on OKVQA. On OCRVQA, Qwen-VL-Chat collects more in-domain data for training, so it performs better than LLaVA-HR. Under the zero-shot setting, we can observe more significant advantages of LLaVA-HR on the fine-grained tasks, *e.g.*, VizWiz and TextVQA. Most notably, even Qwen-VL-Chat is pre-trained with 24.8M OCR samples, it still performs worse than LLaVA-HR-X on TextVQA. These results suggest the significance of high resolution for these tasks. In

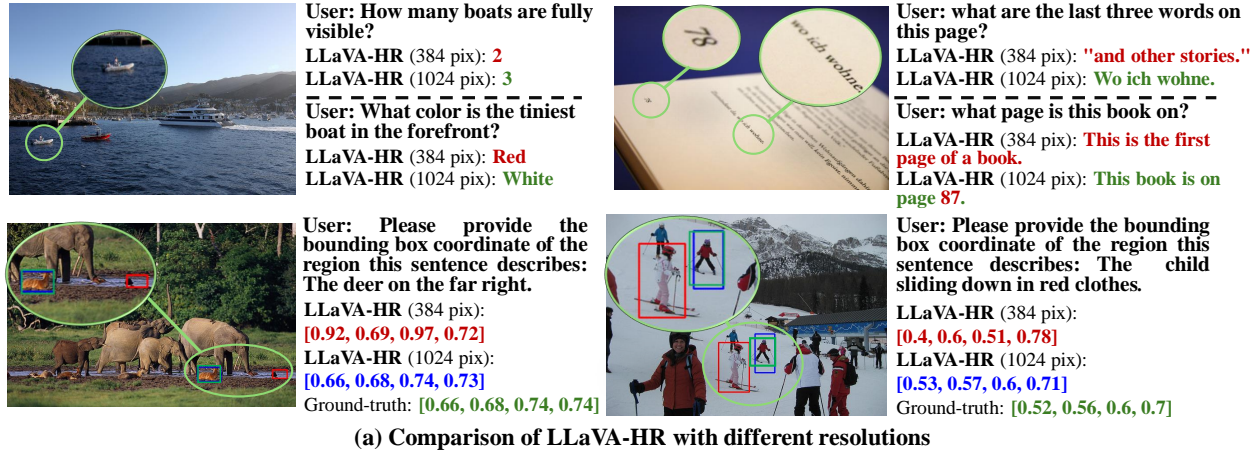


Figure 5. Visualizations of LLaVA-HR and existing MLLMs. Subfig-(a) shows that high image resolution greatly improves the capability of MLLMs on fine-grained VL tasks. In Subfig-(b), LLaVA-HR-X demonstrates the comparable ability with GPT4-V in visual information extraction². Correct and incorrect answers are colored in green and red, respectively.

contrast, most images of ScienceQA are synthetic and of low resolution, so the advantages of LLaVA-HR are not obvious. Overall, these results greatly confirm the effectiveness and generalization of LLaVA-HR and our MRA.

5.3.2. QUALITATIVE EXPERIMENTS

In Fig 5 (a), we compare the predictions of LLaVA-HR with different resolutions. The visualizations show that higher image resolution obviously improves the capability of MLLMs on fine-grained tasks. For example, LLaVA-HR with a resolution of $1,024 \times 1,024$ can well capture granular visual content, e.g., the tiny boat in the first example. Besides, high image resolution also enables LLaVA-HR a stronger ability of text recognition. For instance, the small and blurred phrase of “wo ich wohne” in the second example are correctly identified by the high-resolution LLaVA-HR. These results greatly confirm the significance of high image resolution in addressing visual shortcoming. In Fig 5 (b), we further compare the predictions of LLaVA-HR-X, LLaVA-1.5 (Liu et al., 2023a) and GPT4-V (OpenAI, 2023)

in visual information extraction. Notably, LLaVA-HR-X shows a comparable ability with GPT4-V on this challenging task. As shown in Fig 5 (b), LLaVA-HR-X and GPT4-V can correctly extract almost all visual content of the driver license and organize it in JSON format. Compared to GPT4-V, LLaVA-HR-X also correctly identifies the hair color of the person, which requires fine-grained visual reasoning. In contrast, LLaVA-1.5 can only recognize simple visual content like “class” and “SEX”, and fail to extract most visual information. These results further validate the effectiveness of MRA in addressing visual shortcoming of MLLMs.

6. Conclusion

In this paper, we study the visual shortcoming of MLLMs from the perspective of image resolution, and propose a novel and efficient method for high-resolution adaptations of MLLMs, namely *mixture-of-resolution adaptation* (MRA). MRA adopts dual visual pathways to process images of both high and low resolutions, where high-resolution information is embedded into the low-resolution modeling via the novel *mixture-of-resolution adapters* (MR-Adapters). We

²For privacy reasons, we blur some key personal information.

apply MRA to a popular MLLM called LLaVA-1.5, and construct a new high-resolution MLLM, termed LLaVA-HR. Experimental results not only validate the effectiveness of LLaVA-HR in addressing visual shortcoming, but also confirm its remarkable efficiency against existing MLLMs.

Acknowledgements. This work was supported by National Key R&D Program of China (No.2022ZD0118201), the National Science Fund for Distinguished Young Scholars (No.62025603), the National Natural Science Foundation of China (No. U21B2037, No. U22B2051, No. 62176222, No. 62176223, No. 62176226, No. 62072386, No. 62072387, No. 62072389, No. 62002305 and No. 62272401), the Natural Science Foundation of Fujian Province of China (No.2021J01002, No.2022J06001), and the China Fundamental Research Funds for the Central Universities (Grant No. 20720220068).

References

- Alayrac, J.-B., Donahue, J., Luc, P., Miech, A., Barr, I., Hasson, Y., Lenc, K., Mensch, A., Millican, K., Reynolds, M., et al. Flamingo: a visual language model for few-shot learning. *arXiv preprint arXiv:2204.14198*, 2022.
- Bai, J., Bai, S., Yang, S., Wang, S., Tan, S., Wang, P., Lin, J., Zhou, C., and Zhou, J. Qwen-vl: A frontier large vision-language model with versatile abilities. *arXiv preprint arXiv:2308.12966*, 2023.
- Chen, K., Zhang, Z., Zeng, W., Zhang, R., Zhu, F., and Zhao, R. Shikra: Unleashing multimodal llm’s referential dialogue magic. *arXiv preprint arXiv:2306.15195*, 2023a.
- Chen, T., Kornblith, S., Swersky, K., Norouzi, M., and Hinton, G. E. Big self-supervised models are strong semi-supervised learners. *Advances in neural information processing systems (NeurIPS)*, 33:22243–22255, 2020.
- Chen, X., Wang, X., Changpinyo, S., Piergiovanni, A., Padlewski, P., Salz, D., Goodman, S., Grycner, A., Mustafa, B., Beyer, L., et al. Pali: A jointly-scaled multilingual language-image model. *arXiv preprint arXiv:2209.06794*, 2022.
- Chen, X., Wang, X., Beyer, L., Kolesnikov, A., Wu, J., Voigtlaender, P., Mustafa, B., Goodman, S., Alabdulmohsin, I., Padlewski, P., et al. Pali-3 vision language models: Smaller, faster, stronger. *arXiv preprint arXiv:2310.09199*, 2023b.
- Dai, W., Li, J., Li, D., Tiong, A. M. H., Zhao, J., Wang, W., Li, B., Fung, P., and Hoi, S. Instructblip: Towards general-purpose vision-language models with instruction tuning. *arXiv preprint arXiv:2305.06500*, 2023.
- Dosovitskiy, A., Beyer, L., Kolesnikov, A., Weissenborn, D., Zhai, X., Unterthiner, T., Dehghani, M., Minderer, M., Heigold, G., Gelly, S., et al. An image is worth 16x16 words: Transformers for image recognition at scale. *arXiv preprint arXiv:2010.11929*, 2020.
- Fu, C., Chen, P., Shen, Y., Qin, Y., Zhang, M., Lin, X., Qiu, Z., Lin, W., Yang, J., Zheng, X., et al. Mme: A comprehensive evaluation benchmark for multimodal large language models. *arXiv preprint arXiv:2306.13394*, 2023.
- Fuyu-8B. <https://www.adept.ai/blog/fuyu-8b>, 2023.
- Gilardi, F., Alizadeh, M., and Kubli, M. Chatgpt outperforms crowd-workers for text-annotation tasks. *arXiv preprint arXiv:2303.15056*, 2023.
- Goyal, Y., Khot, T., Summers-Stay, D., Batra, D., and Parikh, D. Making the v in vqa matter: Elevating the role of image understanding in visual question answering. In *Proceedings of the IEEE conference on computer vision and pattern recognition*, pp. 6904–6913, 2017.
- Gurari, D., Li, Q., Stangl, A. J., Guo, A., Lin, C., Grauman, K., Luo, J., and Bigham, J. P. Vizwiz grand challenge: Answering visual questions from blind people. In *Proceedings of the IEEE conference on computer vision and pattern recognition*, pp. 3608–3617, 2018.
- Hudson, D. A. and Manning, C. D. Gqa: A new dataset for real-world visual reasoning and compositional question answering. In *CVPR*, 2019.
- Ilharco, G., Wortsman, M., Wightman, R., Gordon, C., Carlini, N., Taori, R., Dave, A., Shankar, V., Namkoong, H., Miller, J., Hajishirzi, H., Farhadi, A., and Schmidt, L. Openclip. July 2021. doi: 10.5281/zenodo.5143773. URL <https://doi.org/10.5281/zenodo.5143773>. If you use this software, please cite it as below.
- Jiang, H., Misra, I., Rohrbach, M., Learned-Miller, E., and Chen, X. In defense of grid features for visual question answering. In *Proceedings of the IEEE/CVF conference on computer vision and pattern recognition*, pp. 10267–10276, 2020.
- Kingma, D. P. and Ba, J. Adam: A method for stochastic optimization. *arXiv preprint arXiv:1412.6980*, 2014.
- Li, B., Wang, R., Wang, G., Ge, Y., Ge, Y., and Shan, Y. Seed-bench: Benchmarking multimodal llms with generative comprehension. *arXiv preprint arXiv:2307.16125*, 2023a.

- Li, J., Li, D., Savarese, S., and Hoi, S. Blip-2: Bootstrapping language-image pre-training with frozen image encoders and large language models. *arXiv preprint arXiv:2301.12597*, 2023b.
- Li, Y., Du, Y., Zhou, K., Wang, J., Zhao, W. X., and Wen, J.-R. Evaluating object hallucination in large vision-language models. *arXiv preprint arXiv:2305.10355*, 2023c.
- Liu, H., Li, C., Li, Y., and Lee, Y. J. Improved baselines with visual instruction tuning. *arXiv preprint arXiv:2310.03744*, 2023a.
- Liu, H., Li, C., Wu, Q., and Lee, Y. J. Visual instruction tuning. In *NeurIPS*, 2023b.
- Liu, S., Cheng, H., Liu, H., Zhang, H., Li, F., Ren, T., Zou, X., Yang, J., Su, H., Zhu, J., Zhang, L., Gao, J., and Li, C. Llava-plus: Learning to use tools for creating multimodal agents, 2023c.
- Liu, Z., Mao, H., Wu, C.-Y., Feichtenhofer, C., Darrell, T., and Xie, S. A convnet for the 2020s. In *Proceedings of the IEEE/CVF conference on computer vision and pattern recognition*, pp. 11976–11986, 2022.
- Lu, J., Batra, D., Parikh, D., and Lee, S. Vilbert: Pretraining task-agnostic visiolinguistic representations for vision-and-language tasks. *arXiv preprint arXiv:1908.02265*, 2019.
- Lu, P., Mishra, S., Xia, T., Qiu, L., Chang, K.-W., Zhu, S.-C., Tafjord, O., Clark, P., and Kalyan, A. Learn to explain: Multimodal reasoning via thought chains for science question answering. *Advances in Neural Information Processing Systems*, 2022.
- Luo, G., Zhou, Y., Ren, T., Chen, S., Sun, X., and Ji, R. Cheap and quick: Efficient vision-language instruction tuning for large language models. *Advances in neural information processing systems (NeurIPS)*, 2023a.
- Luo, G., Zhou, Y., Sun, J., Sun, X., and Ji, R. A survivor in the era of large-scale pretraining: An empirical study of one-stage referring expression comprehension. *IEEE Transactions on Multimedia*, 2023b.
- Marino, K., Rastegari, M., Farhadi, A., and Mottaghi, R. Ok-vqa: A visual question answering benchmark requiring external knowledge. In *Conference on Computer Vision and Pattern Recognition (CVPR)*, 2019.
- Merigan, W. H. and Maunsell, J. H. How parallel are the primate visual pathways? *Annual review of neuroscience*, 16(1):369–402, 1993.
- Mishra, A., Shekhar, S., Singh, A. K., and Chakraborty, A. Ocr-vqa: Visual question answering by reading text in images. In *2019 international conference on document analysis and recognition (ICDAR)*, pp. 947–952. IEEE, 2019.
- OpenAI. Gpt-4v(ision) system card. https://cdn.openai.com/papers/GPTV_System_Card.pdf, 2023.
- Peng, Z., Wang, W., Dong, L., Hao, Y., Huang, S., Ma, S., and Wei, F. Kosmos-2: Grounding multimodal large language models to the world. *arXiv preprint arXiv:2306.14824*, 2023.
- Radford, A., Kim, J. W., Hallacy, C., Ramesh, A., Goh, G., Agarwal, S., Sastry, G., Askell, A., Mishkin, P., Clark, J., et al. Learning transferable visual models from natural language supervision. *arXiv preprint arXiv:2103.00020*, 2021.
- Ren, T., Liu, S., Zeng, A., Lin, J., Li, K., Cao, H., Chen, J., Huang, X., Chen, Y., Yan, F., Zeng, Z., Zhang, H., Li, F., Yang, J., Li, H., Jiang, Q., and Zhang, L. Grounded sam: Assembling open-world models for diverse visual tasks, 2024.
- Robertson, L. C. and Lamb, M. R. Neuropsychological contributions to theories of part/whole organization. *Cognitive psychology*, 23(2):299–330, 1991.
- Rose, D., Himakunthala, V., Ouyang, A., He, R., Mei, A., Lu, Y., Saxon, M., Sonar, C., Mirza, D., and Wang, W. Y. Visual chain of thought: Bridging logical gaps with multimodal infillings. *arXiv preprint arXiv:2305.02317*, 2023.
- Singh, A., Natarajan, V., Shah, M., Jiang, Y., Chen, X., Batra, D., Parikh, D., and Rohrbach, M. Towards vqa models that can read. In *Proceedings of the IEEE/CVF conference on computer vision and pattern recognition*, pp. 8317–8326, 2019.
- Tong, S., Liu, Z., Zhai, Y., Ma, Y., LeCun, Y., and Xie, S. Eyes wide shut? exploring the visual shortcomings of multimodal llms. *arXiv preprint arXiv:2401.06209*, 2024.
- Touvron, H., Lavril, T., Izacard, G., Martinet, X., Lachaux, M.-A., Lacroix, T., Rozière, B., Goyal, N., Hambro, E., Azhar, F., et al. Llama: Open and efficient foundation language models. *arXiv preprint arXiv:2302.13971*, 2023.
- Yu, J., Li, J., Yu, Z., and Huang, Q. Multimodal transformer with multi-view visual representation for image captioning. *IEEE transactions on circuits and systems for video technology*, 30(12):4467–4480, 2019.

Yu, W., Yang, Z., Li, L., Wang, J., Lin, K., Liu, Z., Wang, X., and Wang, L. Mm-vet: Evaluating large multimodal models for integrated capabilities. *arXiv preprint arXiv:2308.02490*, 2023.

Zhang, P., Li, X., Hu, X., Yang, J., Zhang, L., Wang, L., Choi, Y., and Gao, J. Vinvl: Revisiting visual representations in vision-language models. In *CVPR*, 2021.

Zhu, D., Chen, J., Shen, X., Li, X., and Elhoseiny, M. Minigt-4: Enhancing vision-language understanding with advanced large language models. *arXiv preprint arXiv:2304.10592*, 2023.